

# Performance of QFP Lead-Free Solder Joints Under Dynamic Mechanical Loading

Minna Arra\*, Dongji Xie\*\* and Dongkai Shangguan\*\*

Flextronics

\* Finlaysoninkuja 21 A, 33210 Tampere, Finland

\*\* 2090 Fortune Drive, San Jose, CA 95131, USA

E-mail: minna.arra@fi.flextronics.com

Tel: +358 205 345 411

Fax: +358 205 345 730

This work was originally published in the 2002 Electronic Components & Technology Conference, May 28-31, San Diego, CA.

---

## Abstract

*The performance of Sn/Ag/Cu solder joints with different component lead coating materials (Ni/Pd, 85Sn/15Pb and 98Sn/2Bi) under dynamic mechanical loading was studied in this work using a free fall drop test. PCB substrates with organic solderability preservative (OSP) and immersion gold over electroless nickel (Ni/Au) surface finishes were included in the investigation. Tests were carried out before and after thermal cycling between 0 °C and 100 °C for 3040 cycles. For comparison, lead pull tests were also carried out.*

*It is found from this study that in the as-assembled state, the 98Sn/2Bi coating had the best performance in the drop and pull tests, followed by the 85Sn/15Pb coating. After thermal cycling, a decrease of ~40-50% in the drop test results were seen when compared with the as-assembled state. Failure modes from the drop tests were investigated and the intermetallic compounds (IMC) layer was examined using SEM/EDS to study the impact of IMC on drop test failures.*

---

## Key words

Lead free, solder, reliability, mechanical loading

## 1. Introduction

The fatigue resistance of lead-free solder joints has been shown to be promising from extensively published thermal cycling test results. However, another important reliability

The International Journal of Microcircuits and Electronic Packaging, Volume 24, Number 4, Fourth Quarter, 2001 (ISSN 1063-1674)

© International Microelectronics And Packaging Society

aspect for electronic products, especially handheld products, is the resistance to dynamic mechanical loading, which has not yet been fully understood. From the mechanical point of view, lead-free solder joints may be weaker under dynamic loading such as mechanic shock and drop, as they generally tend to contain more voids. The objective of this study was to investigate the characteristics of the Sn/Ag/Cu solder joints using lead pull and drop tests, with different component lead coatings, before and after accelerated aging of the assemblies.

The previously published results from lead pull tests with Sn/Ag/Cu solder are inconsistent. For example, it was reported that Ni/Pd coated leads give a higher pull strength than those coated with eutectic Sn/Pb solder [1]. In another study, the pull strength of Ni/Pd/Au and Sn/10Pb coated components with the same solder alloy gave equivalent results [2].

Ni/Pd coated QFP lead pull test after thermal cycling test between  $-40^{\circ}\text{C}$  and  $+125^{\circ}\text{C}$  has demonstrated better performance for Sn/Ag/Cu alloy than for eutectic Sn/Pb alloys [3]. The pull strength decreased 10-30% during this thermal cycling test [3]. In another study, the pull strength of QFP leads coated with 90Sn/10Pb and soldered with Sn/Pb and Sn/Ag/Cu alloys has shown no degradation after 5000 cycles of power cycling test between temperatures of  $+25^{\circ}\text{C}$  and  $+100^{\circ}\text{C}$  [4]. Furthermore, the growth of the intermetallic layer thickness between the component and the Sn/Ag/Cu solder during high temperature storage has been found to correlate with the QFP lead pull strength, wa thicker intermetallic layers resulting in a lower lead pull strength [2]. The lead material has also been found to have a significant effect on the pull strength after accelerated aging tests. For example, copper leads have been found to be more favourable than alloy42 leads [4,5].

Voiding, however, has not been found to influence the lead pull strength or solder joint shear strength [4] or to be a reliability problem [6].

---

## 2. Test Vehicle Preparation

Sn/Ag/Cu alloys are expected to be the leading choice of the electronics industry and are recommended by numerous international industry and research consortia. Thus, the 95,5Sn/3,9Ag/0,6Cu (wt-%) alloy was selected for this study, and a commercial solder paste with no-clean, rosin-based, low activity flux was used in the experiments.

A special test vehicle was designed for the study. The overall size of the test substrate was 21,5 cm x 15,1 cm x 1,6 mm. The test vehicle contained 75 different components, and its weight, when fully assembled, was 114 g. This study was focused on the QFP208 type of packages. The daisy-chained QFP208 packages, all having copper leads, were tested with three different lead coating materials: 85%Sn/15%Pb (wt-%), 98%Sn/2%Bi (wt-%), and Ni/Pd. The substrate was designed so that it allowed monitoring of the electrical continuity of the solder joints on each of the component's four sides.

The test substrates were two-layer printed circuit boards (PCB) with conventional FR-4-epoxy as the laminate base material. Two PCB surface finishes were included in the study: organic solderability preservative (OSP) of type Entek 106 and electroless nickel/immersion gold (Ni/Au).

The solder paste was printed on the substrates by using a 125  $\mu\text{m}$  thick stencil. Reflow soldering was carried out in a reflow oven, typically used for high-volume

electronics manufacturing, with eight heating zones and one cooling zone. Reflow was performed in air and the characteristics of the profile experienced by the QFP208 components are presented in Table 1 and Figure 1.

---

### 3. Pull and Drop Test Set-Up

The pull test was performed with Instron 4411 equipment by pulling the leads of the QFP208 packages one by one until failure. A copper wire, 0,23 mm thick, was threaded under the lead, and the ends of the wires were attached to the grip head of the machine. The lead was pulled upwards at 10 mm/min., the board lying at a 45° angle with respect to the vertical direction. The maximum pull force was recorded, and the failure modes were analyzed. The test arrangement is described in Figure 2.

The free fall drop test was carried out with equipment specially assembled for the purpose. In the test set-up, the test vehicle was attached to the drop head with a vacuum suck nozzle. The drop orientation of the sample could be accurately controlled since there are several vacuum nozzles on different sides on the head. At the beginning of the drop, the head together with the sample dropped down from a height of 1.5 m. The vacuum was released after the drop head passed the sensor. This way, only the sample touched the ground and the sample could bounce back freely from the ground. The vehicle was dropped alternately on two of its surfaces as shown in Figure 3. One drop cycle consisted of one drop at each surface. During the drop test, the condition of the solder joints was monitored with electrical measurement from the daisy chain structures. The drop test was continued until the monitored

components dropped off from the board, and afterwards, the failure modes were analyzed.

Pull and drop tests were performed directly after assembly and after an air-to-air thermal cycling test. The thermal cycling test conditions are summarized in Table 2. None of the components tested for pull and drop tests after thermal cycling had failed in the thermal cycling test.

#### 3.1 Pull Test Results

30 measurements were obtained for each combination of component lead coating and PCB surface finish, and the maximum pull force for each individual measurement was recorded. The average result and the standard deviation of the measurements for each lead coating is presented in Figure 4. In the as-assembled state, there were little difference between the tested lead coatings, but the 98Sn/2Bi coating performed slightly better than the other two coatings.

After the thermal cycling test, the pull test values for 85Sn/15Pb coated components decreased by approximately 25%, but the pull test values for the Ni/Pd coated components did not change (Figure 5).

#### 3.2 Drop Test Results

In the as-assembled state, 25 QFPs with 85Sn/15Pb coating and 21 QFPs with 98Sn/2Bi coating were tested. Half of the samples were assembled on boards with OSP and half on boards with Ni/Au surface finish. The number of Ni/Pd coated components tested was only four. The results presented in Figure 6 show the average number of cycles until the component dropped off from the substrate. The trend observed is similar to that for the pull test, i.e. leads with the 98Sn/2Bi coating produced the most reliable joints,

**Table 1. Characteristics of the Reflow Profile.**

Parameter	Value
Pre-heating ramp rate (°C/s)	< 1
Pre-heating profile type	With soak zone
Peak temperature (°C)	241
Time above 217 °C (s)	37

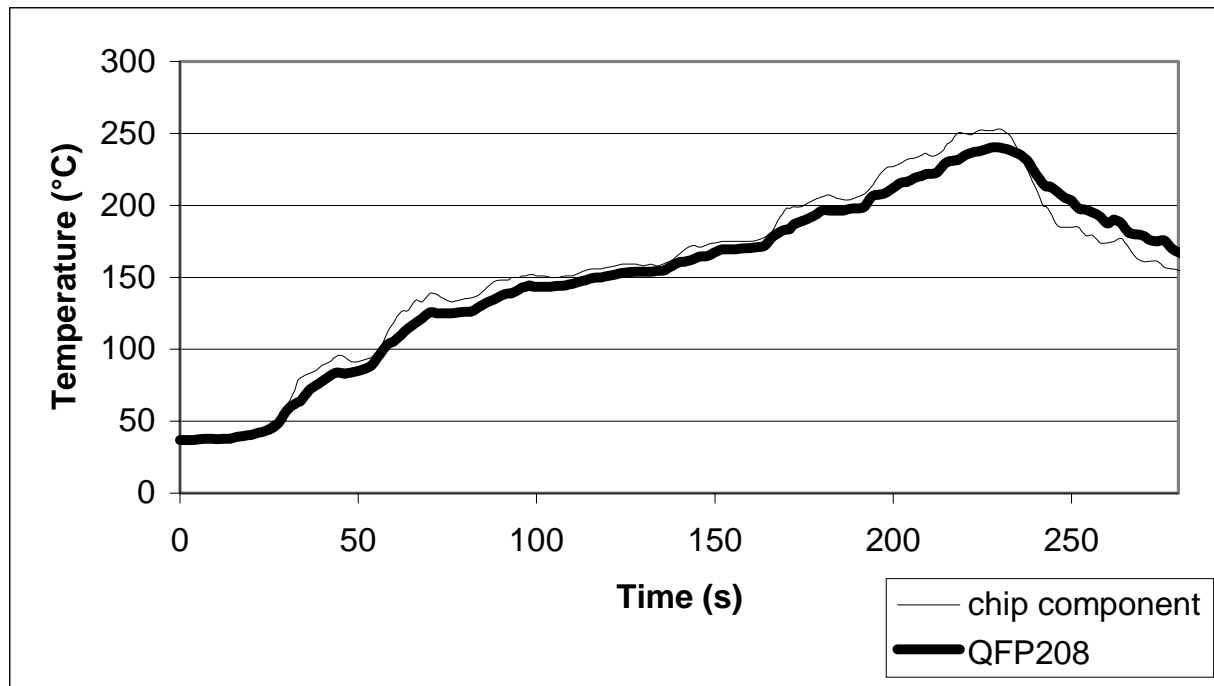


**Figure 1. Reflow Profile Used in the Study.**

and QFP208s with Ni/Pd lead coating had the poorest resistance in the drop test. In most cases, the first electrical failure was observed between 0 and 10 drop cycles. The number of drop cycles to electrical failure and to component drop off correlated well – the earlier the electrical failure was observed, the earlier the component dropped off the board. A typical behavior of the components during the drop test is presented in Figure 7.

Weibull analysis was carried out for 85Sn/15Pb and 98Sn/2Bi coated components, and the results are shown in Figure 8. The two curves are almost in parallel suggesting that 98Sn/2Bi coated QFPs have a higher drop cycles to failure than the 85Sn/15Pb coated components.

After thermal cycling, 16 samples of Ni/Pd and 16 samples of 85Sn/15Pb coated

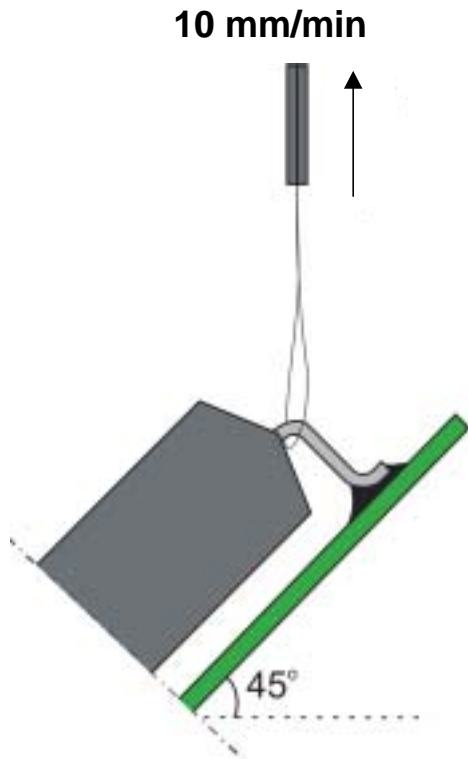


**Figure 2. Pull Test Arrangement.**

components, half of which were assembled on boards with OSP and half on boards with Ni/Au surface finish, were tested. The average number of drop cycles to component drop-off decreased, as compared with the as-assembled state, by 40 % for Ni/Pd and by 54 % for 85Sn/15Pb coated component, respectively, as can be seen from Figure 9. The failure rate for the Ni/Pd coated components is higher than for the 85Sn/15Pb coated components, as can be seen from Figure 10.

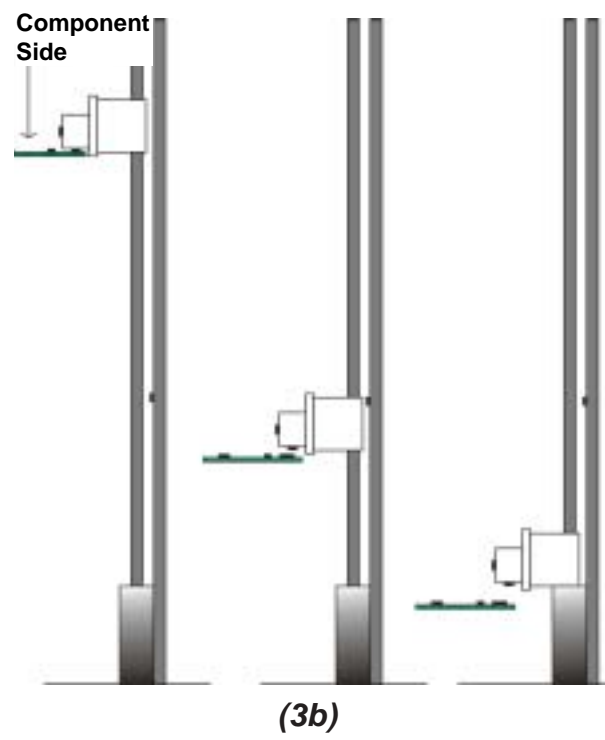
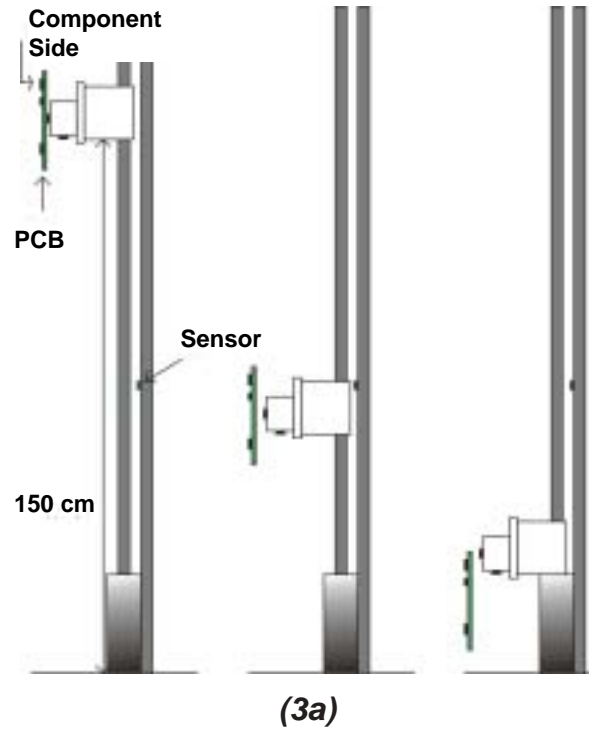


**Figure 3. Drop Test Set-up: One Drop Cycle Included Two Board Orientations; (a) Vertical and (b) Horizontal.**

**Table 2. Air-to-Air Thermal Cycling Test**

<b>Cycle range</b>	<b>Dwell time at extremes</b>	<b>Ramp rate (heating and cooling)</b>	<b>Number of cycles completed</b>
0°C ~ 100°C	10 min	20 °C/min	3040

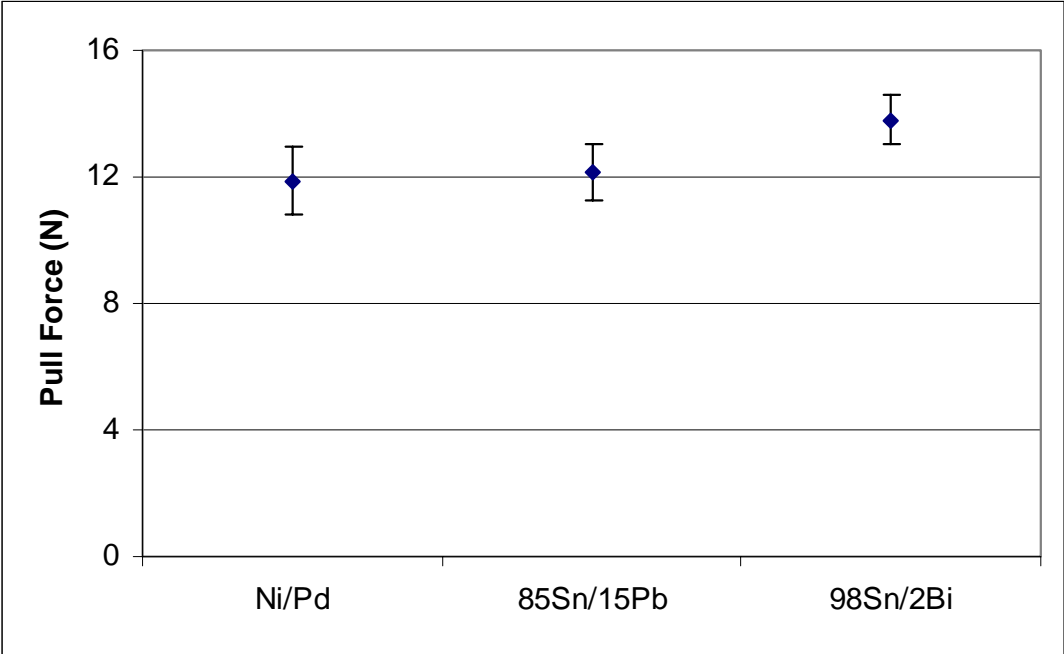


**Figure 4. Pull Test Results after Assembly.**

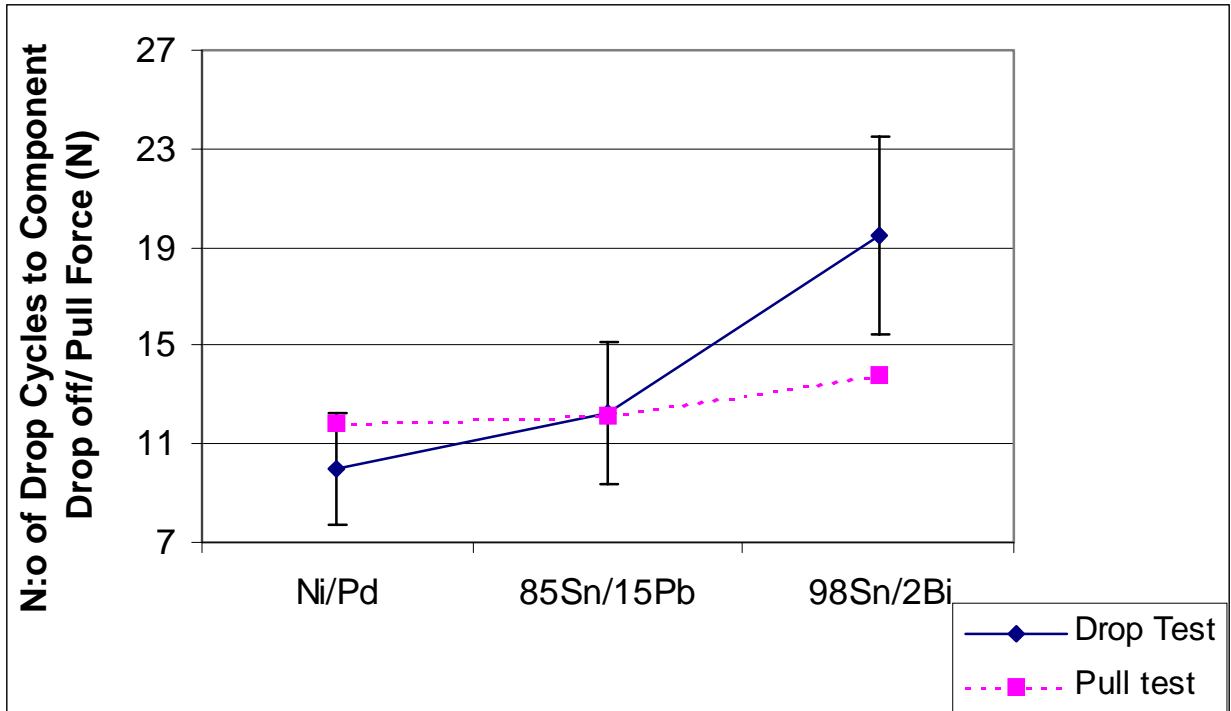


**Figure 5. Pull Test Results after Thermal Cycling Test.**

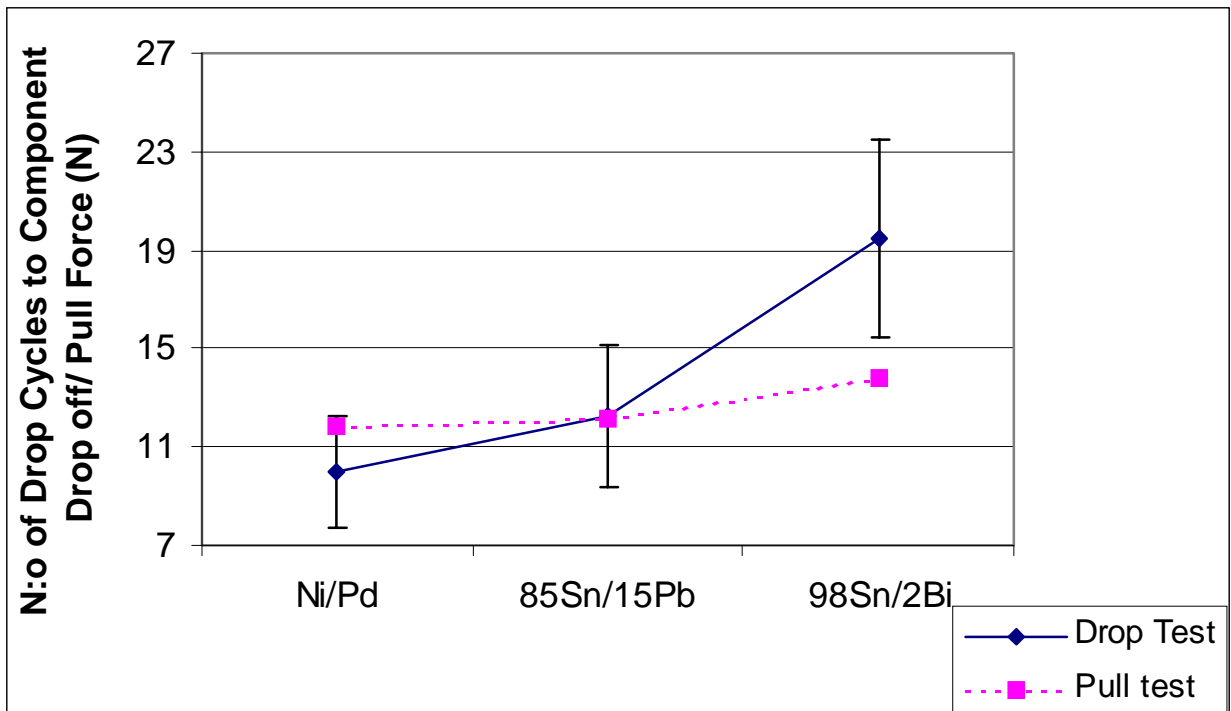


**Figure 6. Drop Test Results after Assembly.**

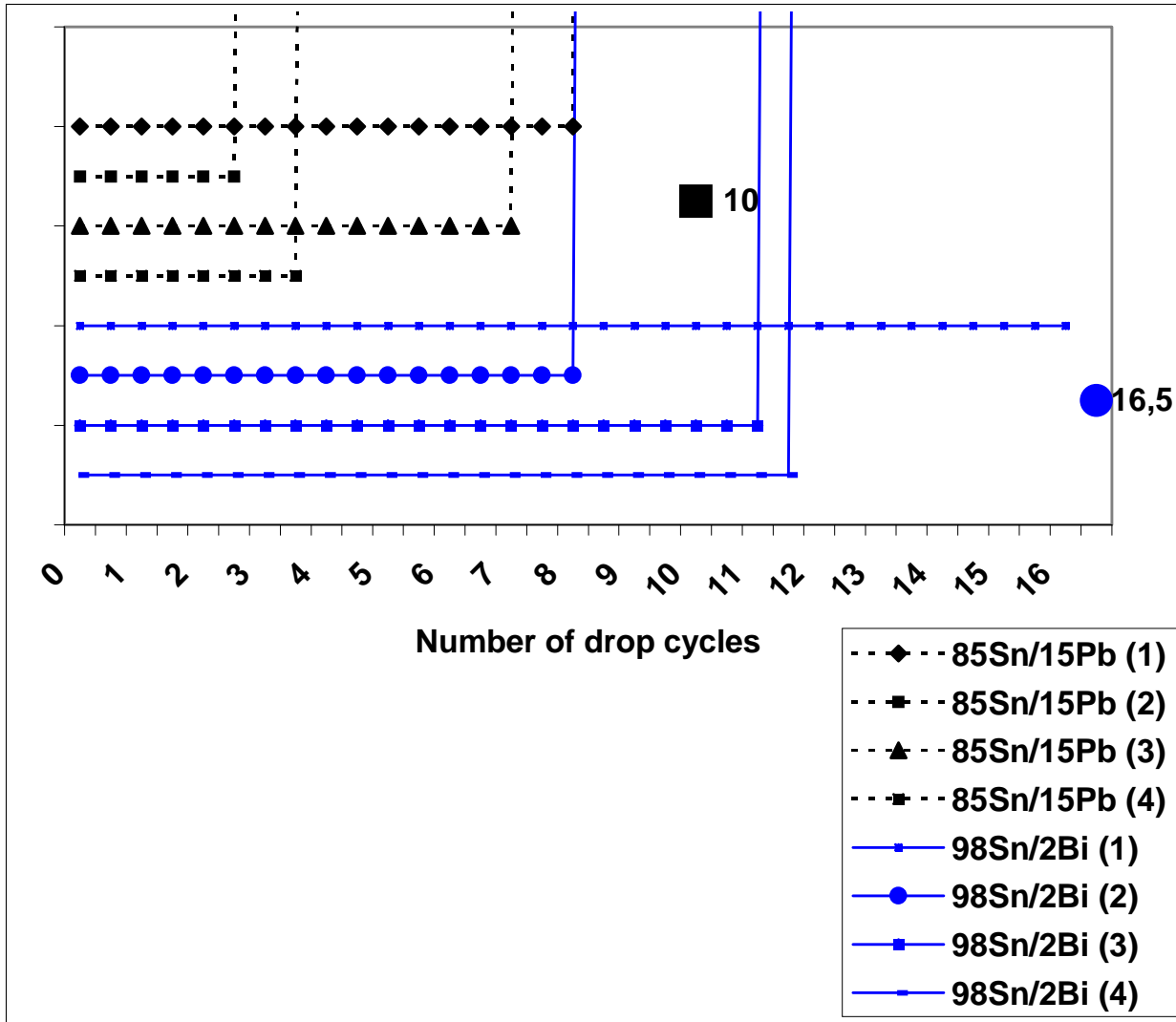


**Figure 7. Typical Example of the Behavior of QFPs During Drop Test. The Dotted Lines Indicate the Electrical Connection in the Four Daisy Chains. The Two Large Dots Indicate the Number of Cycles to Component Drop-off.**

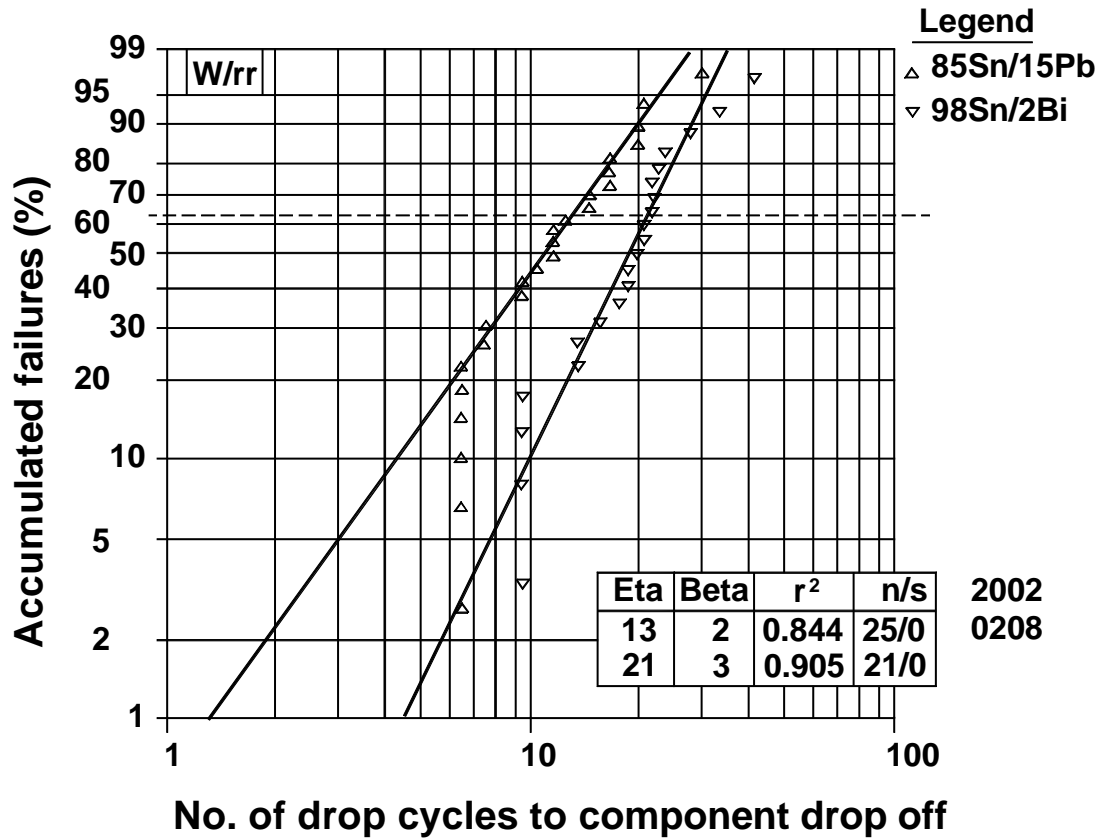


Figure 8. Weibull Chart for 85Sn/15Pb and 98Sn/2Bi Coated Components, after Assembly.

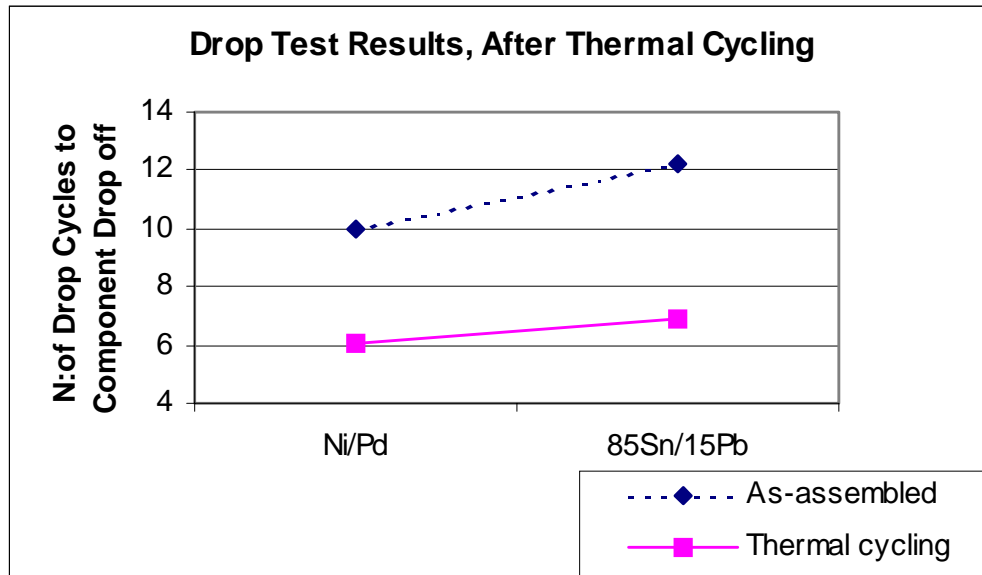


Figure 9. Drop Test Results after Thermal Cycling Test.

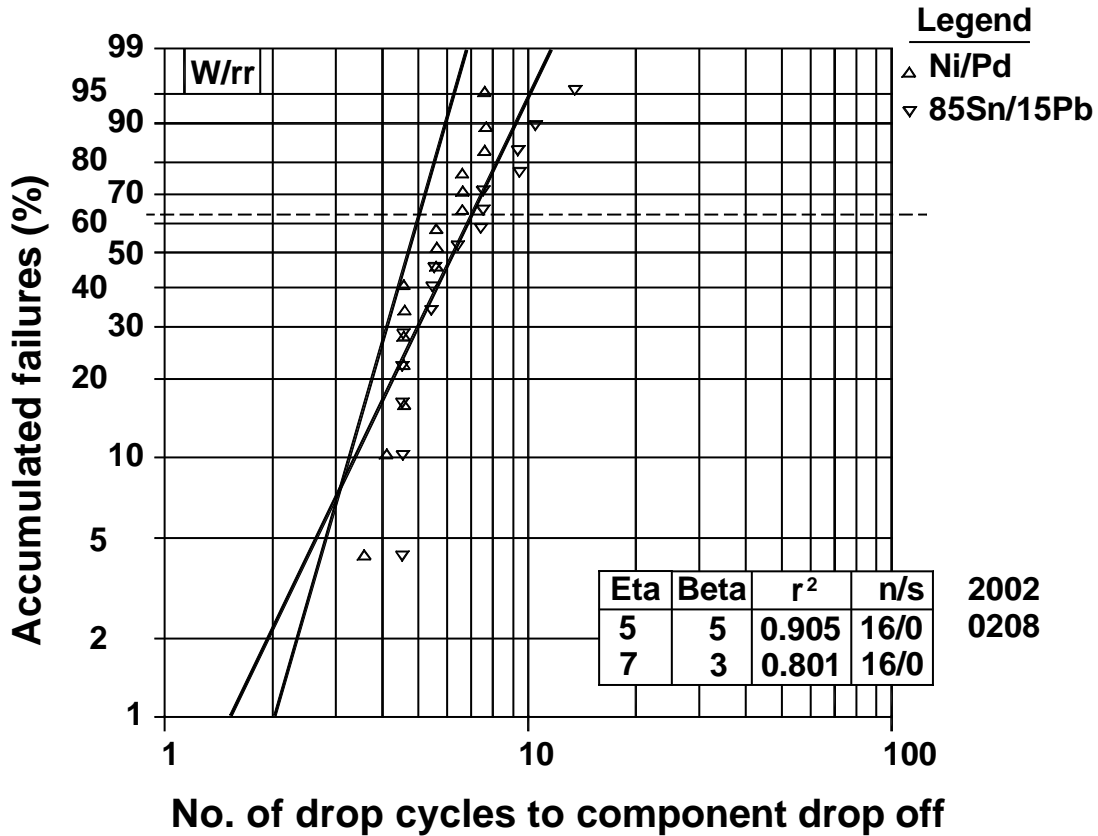


Figure 10. Weibull Chart for 85Sn/15Pb and Ni/Pd Coated Components, after Thermal Cycling Test.

#### 4. Failure Analysis and Discussion

After the pull and drop tests, the failure modes were analyzed, and the failures were categorized into four categories: A) failure partly within the solder, partly within the intermetallic layer between the component and the solder, B) failure within the intermetallic layer between the component and the solder, C) lead rupture and D) pad lifting from the substrate, as shown in Table 3.

In the pull test for the Ni/Pd coated components, the fracture initiated in the solder at the heel fillet, and then proceeded partly

through the solder and partly through the intermetallic layer between the solder and the component as shown in Figure 11a). For Sn/Pb and Sn/Bi coated components, the fracture proceeded through the intermetallic layer as can be seen in Figures 11b) and 11c). The reason for the different path of fracture with the Ni/Pd coated components may be the poorer wetting of the lead, which may locate the stress during the pull test differently, as compared with the 85Sn/15Pb and 98Sn/2Bi coated components.

Voids could often be seen on the fracture surface of the heel fillet part, but were not found to influence the pull strength results.

**Table 3. Major Failure Modes**

			A, %	B, %	C, %	D, %
		<b>Pull Test</b>	<b>As-assembled</b>	<b>Ni/Pd</b>	93	
		<b>85Sn/15Pb</b>		100		
		<b>98Sn/2Bi</b>		100		
	<b>After Thermal Cycling</b>	<b>Ni/Pd</b>	100			
		<b>85Sn/15Pb</b>		100		
<b>Drop Test</b>	<b>As-assembled</b>	<b>Ni/Pd</b>		83	17	
		<b>85Sn/15Pb</b>		80	19	1
		<b>98Sn/2Bi</b>		71	25	4
	<b>After Thermal Cycling</b>	<b>Ni/Pd</b>		82	18	
		<b>85Sn/15Pb</b>		83	17	

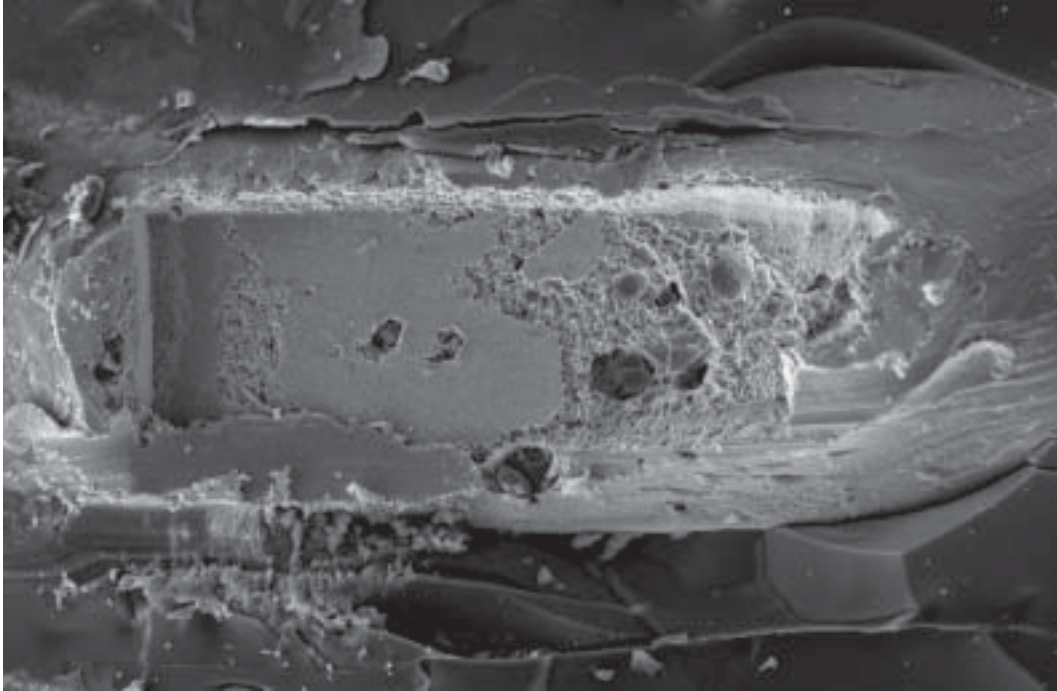
- A: Failure partly within the solder, partly within the intermetallic layer between the component and the solder,
- B: Failure within the intermetallic layer between the component and the solder,
- C: Lead rupture,
- D: Pad lifting from the substrate

After thermal cycling the fracture modes for the Ni/Pd and Sn/Pb coated components remained similar as presented in Figures 11d) and 11e).

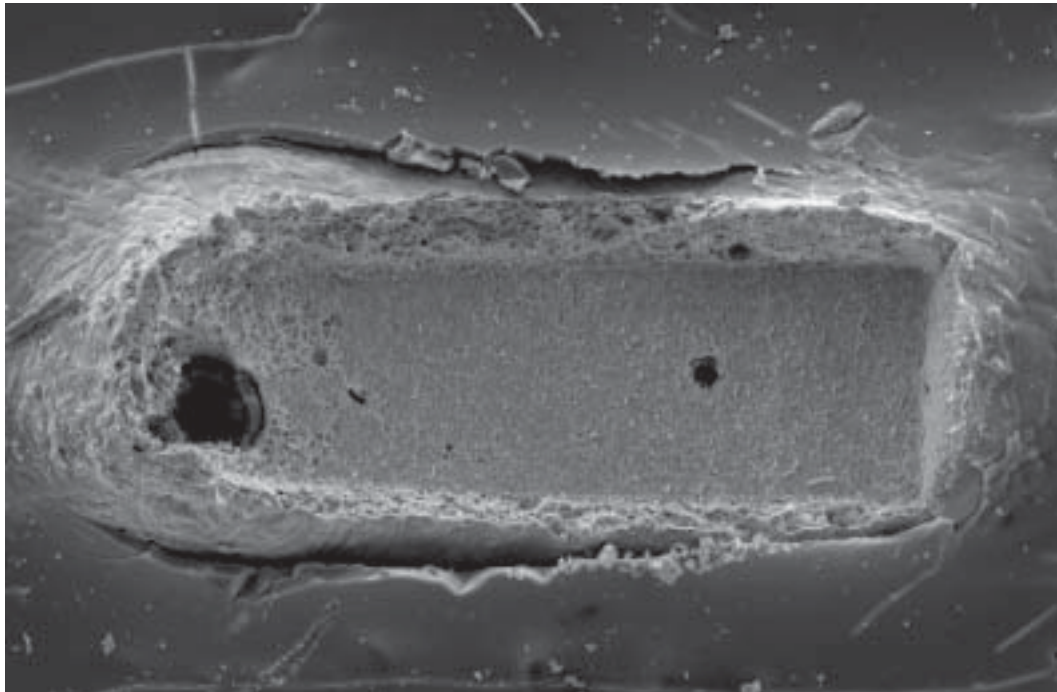
In the drop test, whenever the fracture occurred in the solder joint itself, it was always located in the intermetallic layer between the leads and the solder as shown in Figure 12. This indicates that the intermetallic layer between the leads and solder is the weakest region for this lead type concerning dynamic mechanical shock loading such as drop. In

the drop test, the least solder-lead intermetallic layer failures and the most pad and lead failures for the as-assembled boards were observed for the 98Sn/2Bi coated components as can be seen in Table 3, and the relative number of solder-lead intermetallic failures did not change after the thermal cycling test (Table 3).

The intermetallic layers were studied both from the fracture surfaces and from the cross-section samples, with scanning electron microscope (SEM) and energy dispersive



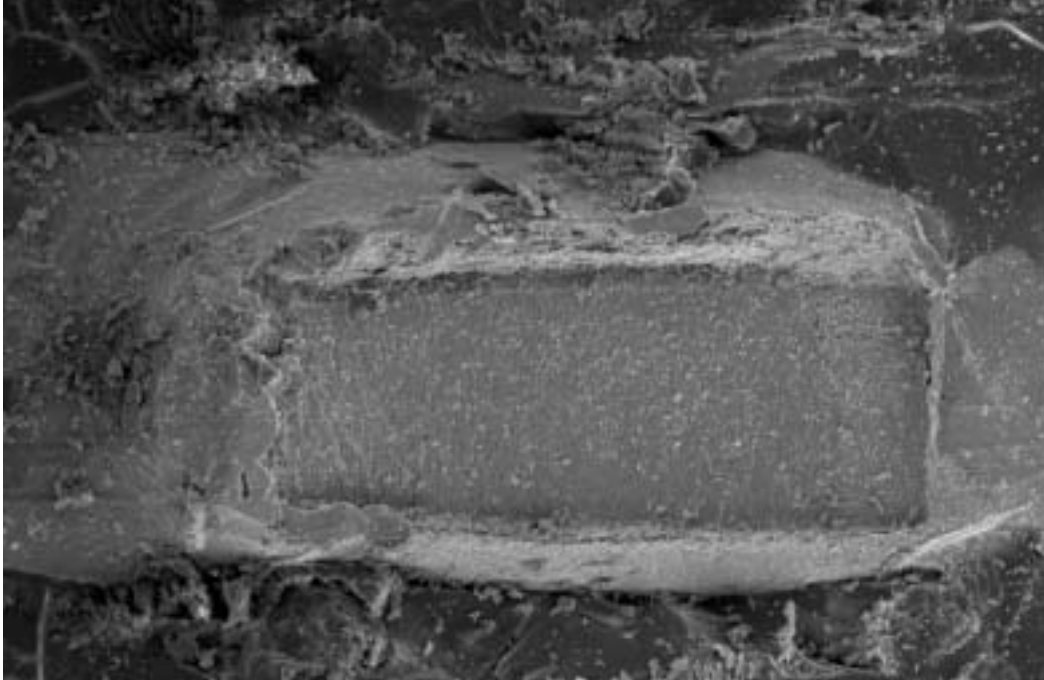
**11a) Ni/Pd, As-assembled**



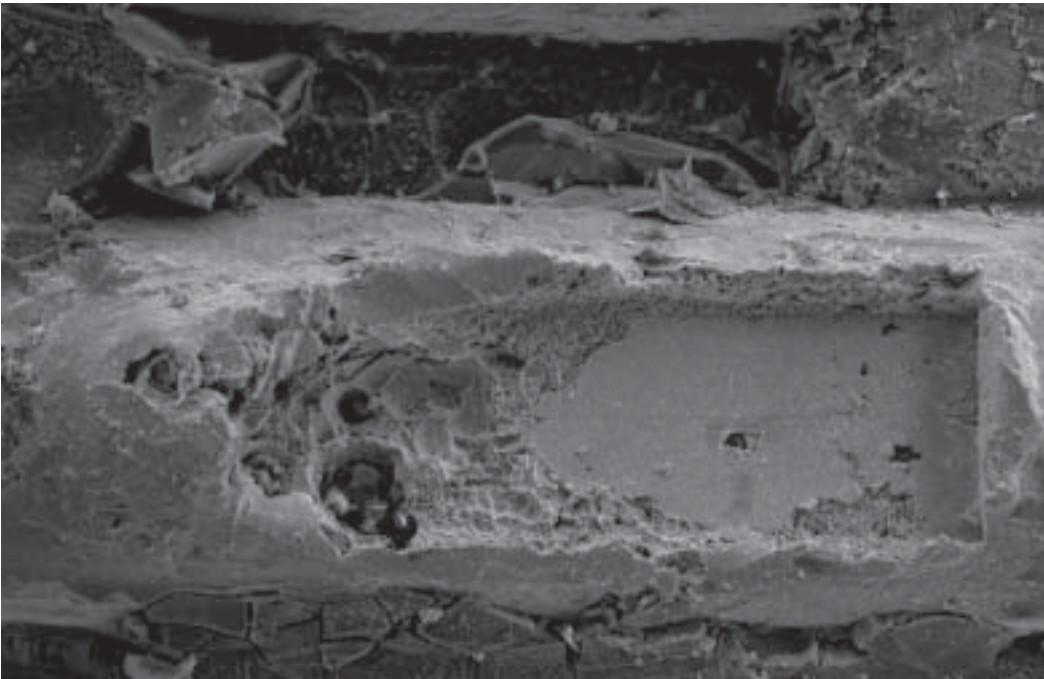
**11b) 85Sn/15Pb, As-assembled**

**Figure 11. The Fracture Surfaces after Pull Test.**

© International Microelectronics And Packaging Society



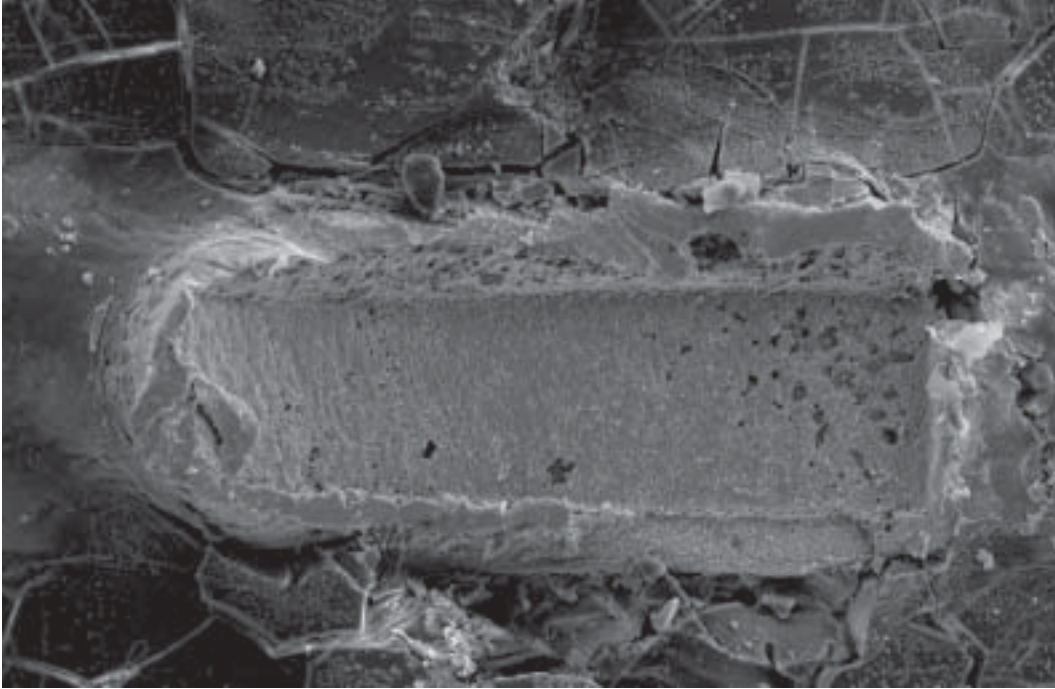
**11c) 98Sn/2Bi, As-assembled**



**11d) Ni/Pd, after Thermal Cycling**

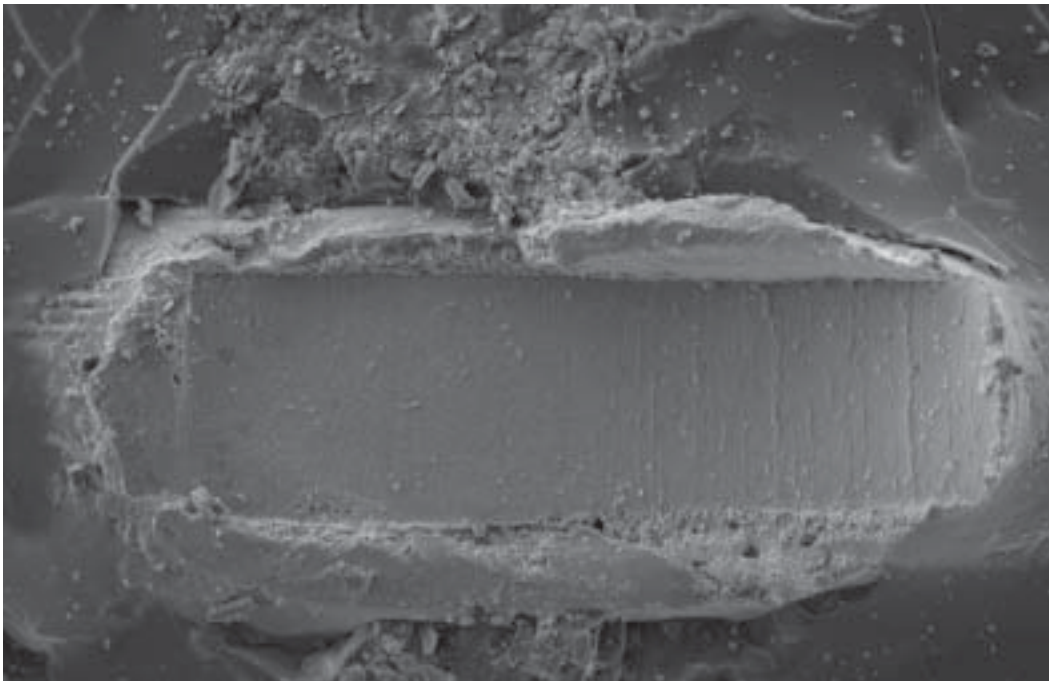
**Figure 11. (Cont.) The Fracture Surfaces after Pull Test.**

© International Microelectronics And Packaging Society



**11e) 85Sn/15Pb, after Thermal Cycling**

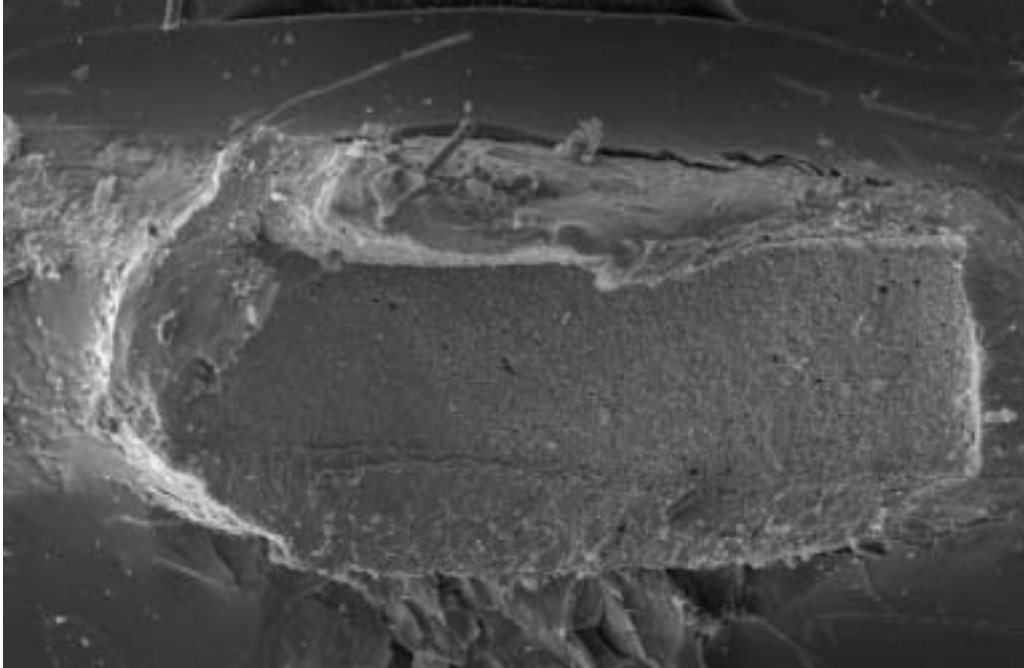
***Figure 11. (Cont.) The Fracture Surfaces after Pull Test.***



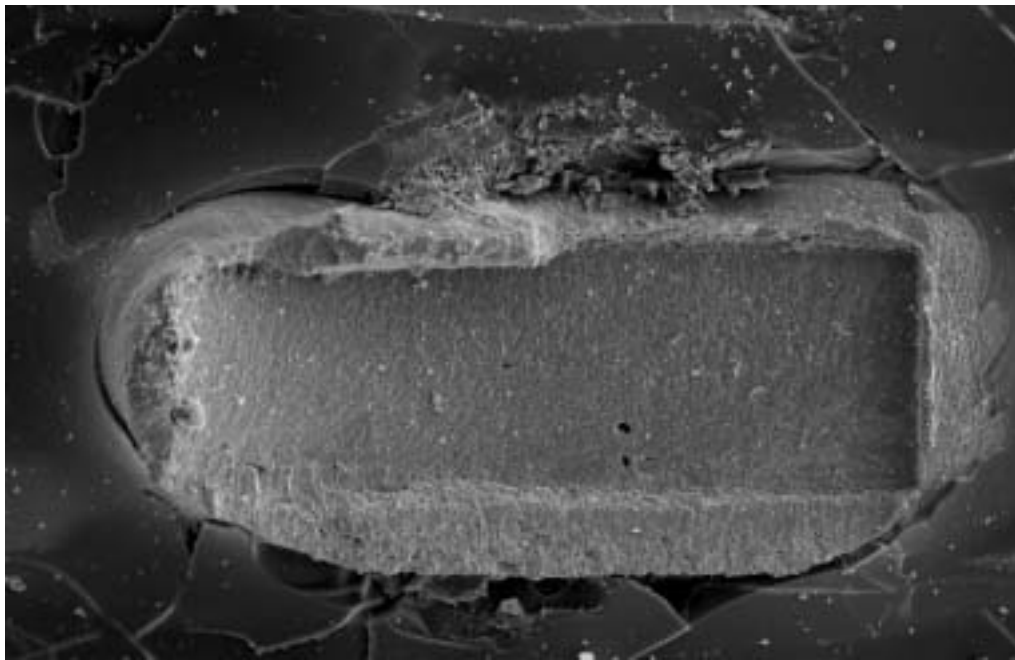
**12a) Ni/Pd, As-assembled**

***Figure 12. The Fracture Surfaces after Drop Test.***

© International Microelectronics And Packaging Society



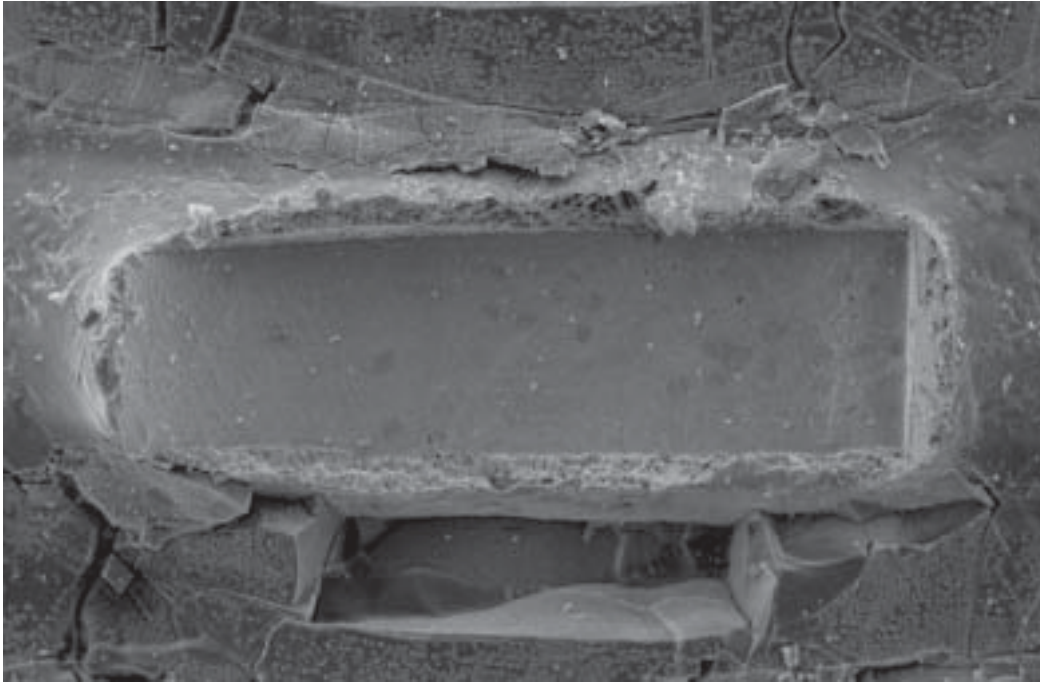
**12b) 85Sn/15Pb, As-assembled**



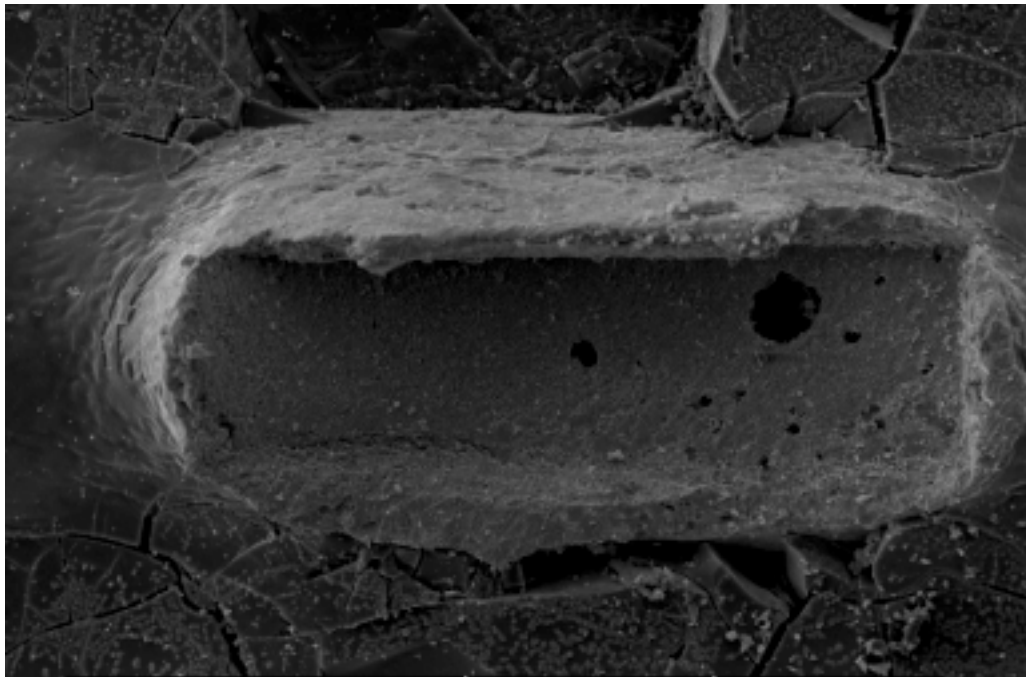
**12c) 98Sn/2Bi, As-assembled**

**Figure 12. (Cont.) The Fracture Surfaces after Drop Test.**

© International Microelectronics And Packaging Society



**12d) Ni/Pd, after Thermal Cycling**



**12e) 85Sn/15Pb, after Thermal Cycling**

**Figure 12. (Cont.) The Fracture Surfaces after Drop Test.**

spectrometer (EDS). The intermetallic layer consisted of  $(\text{Cu, Ni, Pd})_6\text{Sn}_5$  for the Ni/Pd coated components,  $(\text{Cu, Ni})_6\text{Sn}_5$  for the 98Sn/2Bi coated components, and  $(\text{Cu, Ni})_6\text{Sn}_5$  with Pb-rich areas for the 85Sn/15Pb coated components. Nickel in the two latter cases originates from the copper component lead, where it is used as an alloying element. However, the average amount of nickel in the interface with the 85Sn/15Pb and 98Sn/2Bi coated components was only approximately 3 wt-%, whereas with the Ni/Pd coated component it was typically 8-10 wt-%. The silver content in the interface with the Ni/Pd coated components was higher than the nominal silver content in the solder, ranging typically from 3 to 8 wt-%. The intermetallic layer thicknesses between the component and the solder were measured from one sample before and after thermal cycling, as shown in Figure 13. The formation of  $\text{Cu}_3\text{Sn}$  during thermal cycling was not observed. The intermetallic growth during thermal cycling was only slight, if observed at all.

Furthermore, wetting for all of the component types was studied from the cross-section samples. As can be seen from Figure 14, the wetting is poorer for the Ni/Pd coated component, as compared with the 85Sn/15Pb and 98Sn/2Bi coated components.

Since the failures in the drop test were located in the intermetallic layer between the component and the solder, mainly two factors determine the performance of the solder joint in the drop test: the characteristics of the intermetallic layer and the area of the interface, which is in turn determined by the wetting of the component by the solder. The wetting and the intermetallic layer microstructure, except for the existence of Pb-rich phases for the 85Sn/15Pb coated components, is similar for 85Sn/15Pb and 98Sn/2Bi coated components. The

intermetallic layer is slightly thicker for the 98Sn/2Bi coated components than for the 85Sn/15Pb coated components, probably due to the higher amount of Sn in the 98Sn/2Bi coating. It is possible that the presence of Pb in the solder joint may also have made some difference in the pull and drop test performance between these two component types. On the contrary, the reason for the inferior performance of the Ni/Pd coated components in the drop test may be attributed to the different composition of its intermetallic layer but also to the wetting, which is considerably poorer than for the 85Sn/15Pb and 98Sn/2Bi coated components.

The results between the pull and drop tests before and after thermal cycling correlated fairly well for the 85Sn/15Pb and 98Sn/2Bi components. For the Ni/Pd coated components, the pull test results were better than would be expected based on the drop test results, probably due to the different failure mechanisms between the pull test and the drop test for these components.

The drop test performance of both 85Sn/15Pb and Ni/Pd coated components after the exposure to the thermal cycling test may not be determined only by the intermetallic layer thickness, but also by the solder matrix microstructure, such as grain coarsening or microcracking. Future work is needed to understand the failure mechanisms.

---

## 5. Conclusions

A new free fall drop test, simulating typical stresses experienced by portable devices, has been investigated. The results show that the best performing solder joints in the as-assembled state, both in the drop and pull tests, were obtained with the 98Sn/2Bi coated

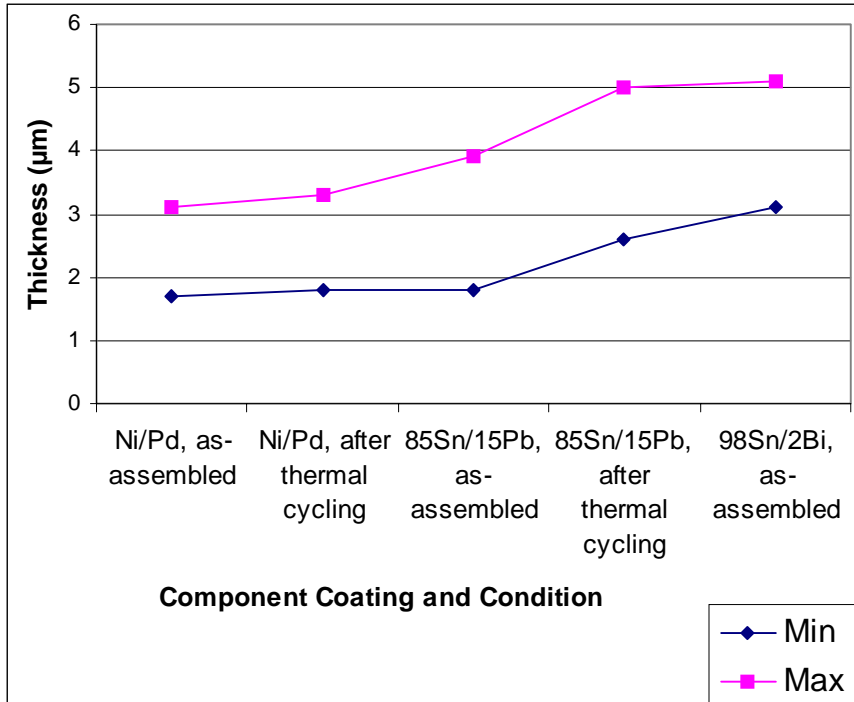
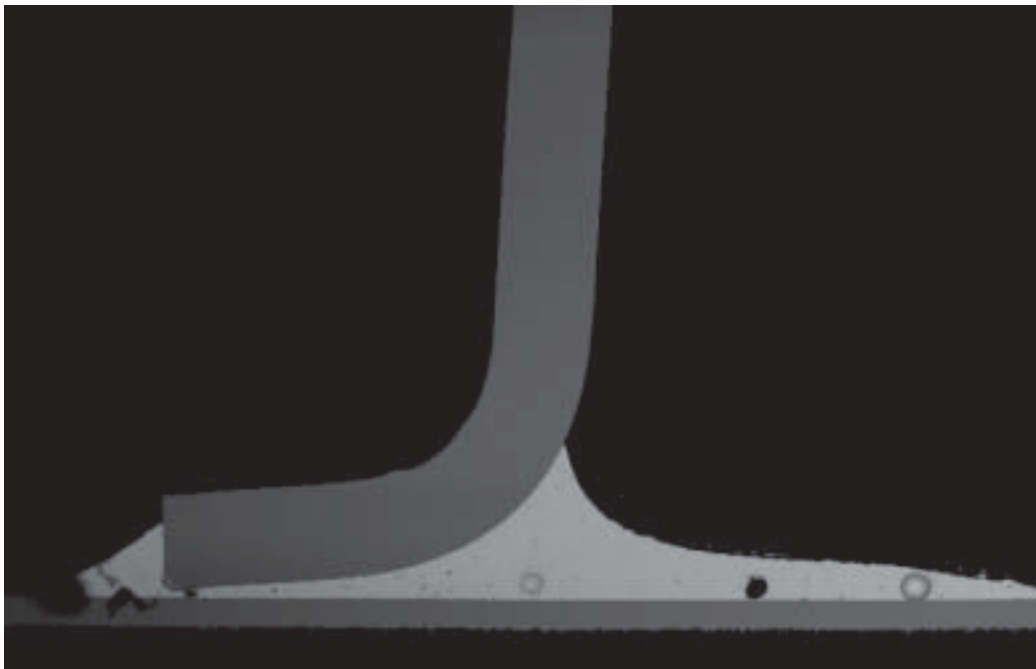
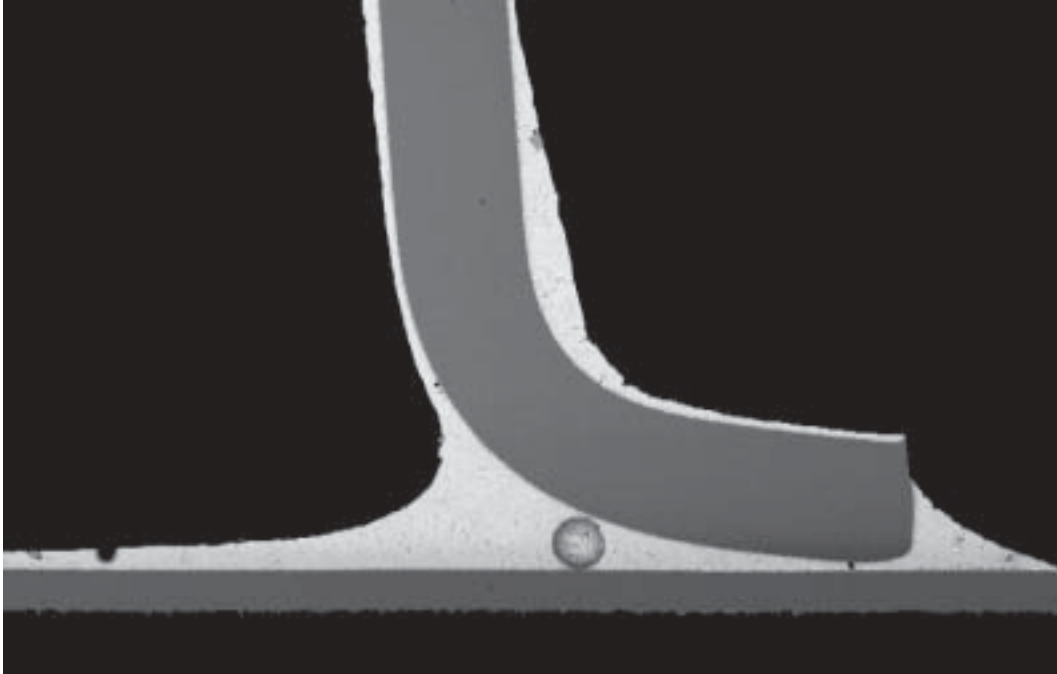


**Figure 13. Intermetallic Layer Thicknesses.**

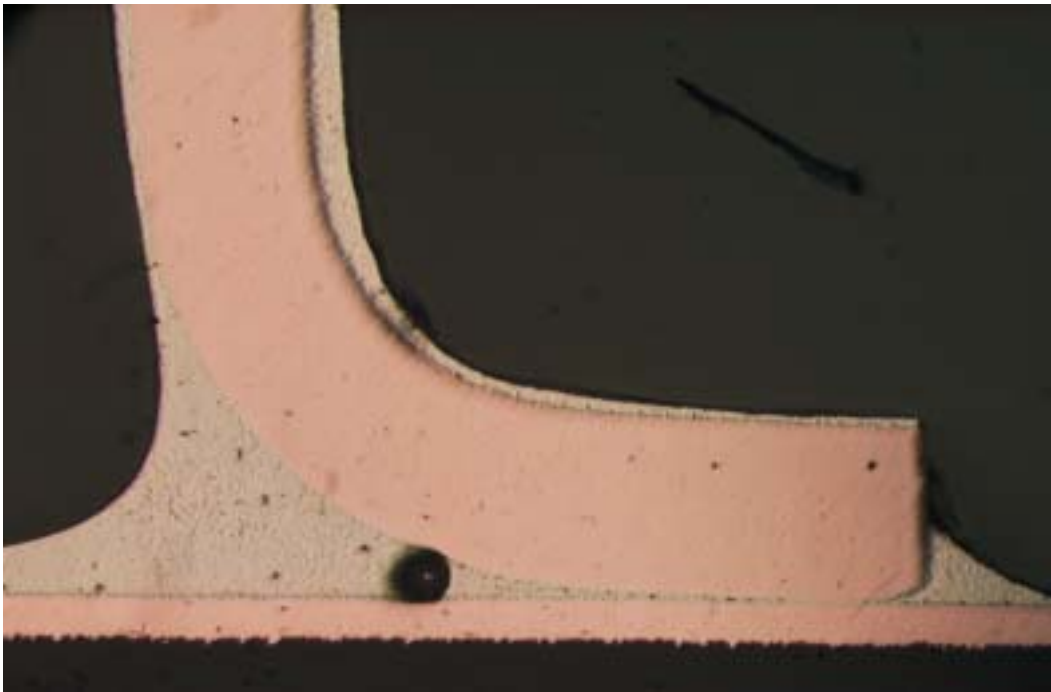


**(14a)**

**Figure 14. The Wetting of the Components by the Solder.**



(14b)



(14c)

*Figure 14 (Cont.). The Wetting of the Components by the Solder.*

© International Microelectronics And Packaging Society

components. Between the two other coatings studied, 85Sn/15Pb and Ni/Pd, 85Sn/15Pb coating gave slightly better results in the drop test. In general, the correlation between the pull and drop tests was found to be fairly good.

After thermal cycling between 0 °C and 100 °C for 3040 cycles, both Ni/Pd and 85Sn/15Pb coated components resulted in 40-50% lower performance in the drop test, due to degradation in the solder joints during the thermal cycling. The failure mode in the drop test is brittle and the failures occur in the intermetallic layer between the component and the solder.

---

## Acknowledgments

The authors would like to thank Janne Sundelin at Tampere University of Technology for his help in the pull testing and SEM analysis.

---

## References

1. Y. Tsunematsu, et al., "Evaluation of Pb-Free Solders for Adaptability to Various Soldering Processes", *Proceedings of EcoDesign '99: First International Symposium on Environmentally Conscious Design and Inverse Manufacturing*, Tokyo, Japan, February, 1999, pp. 610-614
2. A. Hirose, et al., "Influence of Interfacial Reaction on Reliability of QFP Joints with Sn-Ag Based Pb Free Solders", *Materials Transactions*, Vol. 42, No. 5 (2001), pp. 794-802.

3. D. Romm, et al., "Evaluation of Nickel/Palladium –Finished ICs With Lead-Free Solder Alloys", Application report SSZA024, January, 2001, available at <http://www.ti.com/sc/docs/products/leadfree/appnotes.htm>.

4. F. A. Stam, et al., "Effects of Thermomechanical Cycling on Lead and Lead-Free (Snpb and Snagcu) Surface Mount Solder Joints", *Microelectronics Reliability*, Vol. 41 (2001), pp. 1815-1822.

5. M. R. Harrison, et al., "Lead-free Reflow Soldering For Electronics Assembly", *Soldering & Surface Mount Technology*, Vol. 13, No. 3 (2001), pp. 21-38.

6. C. Olsson, "Reliability of Lead-free Solder Connections", Ericsson internal document, ERA/SRV-01:0036 Uen Rev: B, 2001